DOI: 10.1002/cphc.200600511

Geometric H/D Isotope Effects and Cooperativity of the Hydrogen Bonds in Porphycene

Mohamed F. Shibl,[a] Mariusz Pietrzak,[b] Hans-Heinrich Limbach,[a] and Oliver Kühn*[a]

We investigate the primary, secondary, and vicinal hydrogen/deuterium (H/D) isotope effects on the geometry of the two intramolecular hydrogen bonds in porphycene. Multidimensional potential energy surfaces describing the anharmonic motion in the vicinity of the trans *isomer are calculated for the different symmetric (HH/DD) and asymmetric (HD) isotopomers. From the solution of the nuclear Schrödinger equation the ground-state wavefunction is obtained, which is further used to determine the quantum corrections to the classical equilibrium geometries of the hydrogen bonds and thus the geometric isotope effects. In particular, it is found that the hydrogen bonds are cooperative, that is, both expand simultaneously even in the case of an asymmetric isotopic substitution. The theoretical predictions compare favorably with NMR chemical-shift data.*

Introduction

Isotopic substitution provides a rather specific way of obtaining information on the nature of potential energy surfaces (PES) and molecular wavefunctions.[1] Observables showing isotope effects include NMR chemical shifts reflecting structural properties and equilibrium constants,[2–6] rate constants of reaction kinetics[7] or cross-sections in reaction dynamics.[8] Isotope effects are especially pronounced when quantum tunneling is of importance, such as in the case of low-temperature reactions involving the motion of hydrogen/deuterium atoms. As a matter of fact, this is one of the few instances where quantum mechanics surfaces, even in complex biological systems (see, e.g. refs. [9, 10]), but also the influence on the structure, that is, the geometric isotope effect (GIE), is of quantum mechanical origin. Consider the linear A–H···A hydrogen bond (HB) in Figure 1 a, which is defined by the two distances r_1 and r_2, or alternatively, by the coordinates $q_1=(r_1-r_2)/2$ and $q_2=r_1+r_2$. Figure 1 b shows effective one-dimensional potentials for the H and D motion for fixed values of q_2.[3, 11, 12] As a consequence of the potential's anharmonicity and the different zero-point energies of the ground-state wavefunctions $\Psi(H)$ and $\Psi(D)$, a local probe of the average position will detect a smaller A–D distance as compared to the A–H distance (primary GIE). Moreover, both distances differ from the predictions of the equilibrium distance within a classical nuclei approach as it is obtained, for example, from a standard quantum chemical geometry optimization.

In addition, the shape and height of the barrier of the one-dimensional potential may be different for the two cases, indicating the interdependence between geometric and kinetic isotope effects. This is where the correlation between the H/D (q_1) and the heavy atom A···A (q_2) motion comes into play.

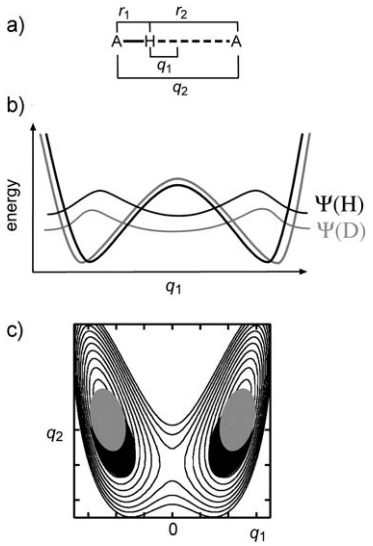

Figure 1. a) Linear hydrogen bond with the distances r_1 and r_2 as well as the definition of q_1 and q_2. b) Schematic effective one-dimensional potentials and ground-state vibrational functions for hydrogen (black) and deuterium (grey). c) Schematic view of the ground-state wavefunction for hydrogen (black) and deuterium (grey) in a two-dimensional potential surface incorporating q_1 and q_2 of panel (a).

[a] *Dr. M. F. Shibl, Prof. H.-H. Limbach, Dr. O. Kühn*
Institut für Chemie und Biochemie
Physikalische und Theoretische Chemie
Freie Universität Berlin, Takustr. 3
14195 Berlin (Germany)
Fax: (+49) 3083854792
E-mail: ok@chemie.fu-berlin.de

[b] *Dr. M. Pietrzak*
Institute of Physical Chemistry
Polish Academy of Sciences
Kasprzaka 44/52, 01-224 Warsaw (Poland)

Viewed from a two-dimensional quantum perspective, as sketched in Figure 1c, the coupling between q_1 and q_2 leads to a PES which results in a ground-state wavefunction tilted with respect to the coordinate axes. In this picture, isotopic H/D substitution causes a simultaneous motion along q_1 and q_2, that is, the local maxima of the distribution shift to larger absolute values of these coordinates. In other words, the HB expands, that is, it is weakened. This so-called secondary GIE on the HB distance q_2 was first investigated for molecular crystals using X-ray crystallography by Ubbelohde and Gallagher (Ubbelohde effect).[13] It was only recently, that Benedict et al. showed that primary and secondary GIEs in N···H–N HBs can be obtained as well from solid-state ^{15}N NMR measurements.[3]

In the present Article we give a theoretical account on the GIE of an intramolecular double HB. Multiple HBs continue to attract considerable attention, not least because of their prominent role in biological systems.[14] An issue of principal importance concerns the question whether H dynamics in multiple HBs takes place concertedly or by means of uncorrelated individual steps. NMR relaxometry measurements may give evidence for the preferred mode of transfer as shown, for example, in refs. [15, 16]. At this point, one may ask whether the GIE contains such information as well. It has been shown for the intermolecular HB in the acetic acid dimer that the GIE indicates cooperativity of the two HBs.[17] Cooperativity implies that isotopic substitution in one HB leads to a geometric change in the other HB, which goes into the same direction, that is, both HBs may contract or expand. To bring this into the context of H transfer, consider an intramolecular double HB as shown in Figure 2. A concerted double H transfer requires the molecular scaffold to follow the motion in such a way as to provide a simultaneous contraction of both HBs. Conversely, in a stepwise process, the molecular rearrangement is likely to be non-symmetric. The same would hold for a double D transfer. The following question arises: what happens upon single deuteration (HD case)? One may argue that the asymmetry introduced by the different masses will make the transfer stepwise in any case. On the other hand, if the preferred mode of scaffold rearrangement is of the symmetric type, this might still be observed notwithstanding the perturbation of the symmetry due to H/D substitution. In other words, the HBs are cooperative and thus the GIE may give strong indication for the transfer mechanism in a double HB.

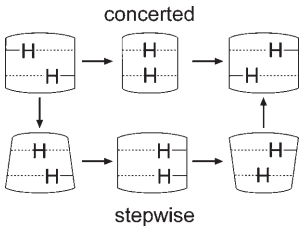

Figure 2. Sketch of concerted (upper path) and stepwise (lower path) double H atom transfer and its relation to the likely rearrangement of the molecular skeleton.

In a first step to assess this working hypothesis we have studied the GIE in the intramolecular double-HB system porphycene shown in Figure 3. Porphycene has been synthesized by Vogel et al.[18] as a constitutional isomer of porphin. As compared to the latter, it provides a tighter cavity for the two H atoms which enhances the strength of the HBs. This statement is supported by X-ray diffraction,[18] infrared,[19] and NMR spectroscopy[20] (for a review, see also ref. [21]). From the theoretical point of view, porphycene is an example for a system exhibiting a Hartree–Fock instability. This issue was addressed by Hohlneicher and co-workers who showed that Hartree–Fock theory predicts an electronic ground state of low symmetry with pronounced bond-length alternations. This failure can only be compensated by accounting for electron correlations, for example, at the level of density functional theory (DFT).[22] Although the infrared spectrum could not give clear evidence for the most stable isomer,[19] quantum chemical calculations indicate that the *trans* isomer shown in Figure 3 is the most stable form (see also ref. [23]).

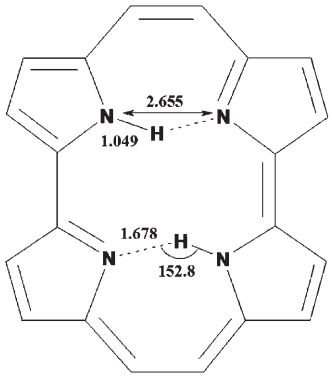

Figure 3. The DFT(B3LYP)/6-31G(d,p) optimized geometry of a *trans* isomer of porphycene. Notice that the N–N distance and the N–H–N angle are in fair agreement with the experimental values of 2.63 Å[18] and 152°.[16]

The theoretical prediction of the GIE requires the calculation of the wavefunction for the nuclei involved in the HBs. In this case one usually resorts to the Born–Oppenheimer separation of electronic and nuclear coordinates restricted to the electronic ground state. In principle, one needs to obtain a PES along relevant coordinates for which the nuclear Schrödinger equation can be solved (see, for example, refs. [3, 5, 11, 24]). Alternatively, the PES can be generated on the fly along with a molecular dynamics simulation[25] or the standard Born–Oppenheimer separation can be abandoned by treating the proton/deuteron on the same footing as the electrons. The latter, so-called multicomponent, approach is computationally very demanding. For molecules of the size of porphycene further approximations are required, degrading the quality of the quantum chemistry.[26]

Herein, we present multidimensional nuclear wavefunction calculations of the HH/HD/DD primary and secondary GIE in porphycene. In the following section we extend our previous study of the HH/DD GIE in porphycene[26] and derive reduced-dimensionality Born–Oppenheimer PES based on explicit two-dimensional quantum chemical calculations supplemented by third-order anharmonic couplings for the different isotopom-

ers. The expectation values for the atomic positions are extracted from the respective four- (4D, HH and DD case) and six-dimensional (6D, HD case) nuclear ground-state wavefunctions. Subsequently, the predicted GIEs are compared with NMR data and implications for the cooperativity of the double HB in porphycene are addressed.

Computational Methods

We consider the behavior of the nuclear ground-state wavefunction of porphycene in the vicinity of a *trans* geometry (see Figure 3) on the Born–Oppenheimer PES. For all quantum chemical calculations we used the DFT/B3LYP method in combination with a 6-31G(d,p) basis set as implemented in Gaussian 03.[27] The above-mentioned restriction to a single nuclear configuration neglects—of course—the influence of the tunneling coupling between the two *trans* minima. However, since the tunneling splitting, as determined from fluorescence excitation spectra, is relatively small (4.3 cm^{-1}),[28] there should be only a marginal effect on the shape of the local probability density. This approximation has been checked by two-dimensional model calculations, which include the coordinates of the concerted motion of the two hydrogen atoms in a relaxed molecular scaffold.[29]

This allows us to express the vibrational Hamiltonian in the Watson form[30] by means of the $3N-6$ mass-weighted normal-mode coordinates, $\{Q_i\}$, of a C_{2h} *trans* configuration ($N=38$ for porphycene). If $\{P_i\}$ denotes the set of conjugate momenta, and provided that rotation is neglected, one has [Eq. (1)]:

$$H=\sum_i \frac{P_i^2}{2}+\sum_i V^{(1)}(Q_i)+\sum_{i<j} V^{(2)}(Q_i,Q_j)+\sum_{i<j<k} V^{(3)}(Q_i,Q_j,Q_k) \quad (1)$$

Notice that the potential-energy part involves an approximation, since the full potential is expressed in terms of one-, two-, and three-mode correlation potentials as indicated by the superscripts.[31] Notice further that due to the mass-weighting of the coordinates, a PES has to be determined for each isotopomer.

The selection of relevant coordinates starts from the symmetric ($Q_1^{HH/DD}$) and antisymmetric ($Q_2^{HH/DD}$) N–H(D) stretching vibrations, the former is shown in Figure 4a. In a preliminary investigation[26] we identified a strongly coupled low-frequency mode ($Q_4^{HH/DD}$) for the HH and DD case by displacing the molecular geometry along $Q_1^{HH/DD}$ and $Q_2^{HH/DD}$ and calculating the force exerted on all other normal modes. The displacement vector of this strongly coupled mode is shown in Figure 4d. Apparently, this promoting-type mode causes a symmetric contraction of the two HBs, that is, it is strongly related to the secondary GIE. In passing we note that this low-frequency mode has also been used to explain temperature-dependent tautomerization rates.[21] Taking these three modes we determined a PES on a numerical grid incorporating up to two mode correlations in Equation (1). To refine this model we have calculated third-order force constants, K_{ijk}, using the combination of analytical Hessians and finite differencing, as proposed in ref. [32]. It turns out that in both cases, HH and DD, there is an additional important coupled mode ($Q_3^{HH/DD}$), at around $\approx$900 cm^{-1}, whose displacement vectors are shown in Figures 4b (HH) and 4c (DD). Displacement along this mode lowers the symmetry and allows for asynchronous contraction/elongation of the two HBs. There are no diagonal third-order force constants for this mode, however, there is a particularly strong three-mode correlation with the stretching vibrations, $K_{123}^{HH}=-224$ cm^{-1} and $K_{123}^{DD}=-197$ cm^{-1}, as well as a weaker coupling with the antisymmetric stretching and the low-frequency vibration, $K_{234}^{HH}=-35$ cm^{-1} and $K_{234}^{DD}=-24$ cm^{-1}. All other couplings do not exceed 10 cm^{-1}. Keeping the harmonic approximation for mode $Q_3^{HH/DD}$ and combining it with the explicit two-mode potentials for modes $Q_1^{HH/DD}$, $Q_2^{HH/DD}$, and $Q_4^{HH/DD}$ as well as the third-order anharmonic couplings mentioned before, we arrive at a 4D model for the HH and DD cases.

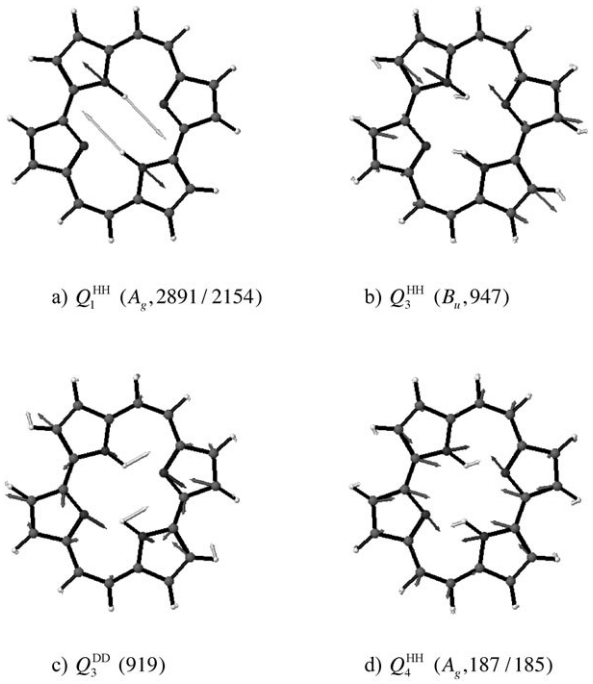

Figure 4. Selected normal-mode displacement vectors entering the 4D model for the HH and DD cases. The harmonic frequencies are given in parenthesis (HH/DD in cm^{-1}). The DD modes that are not shown are rather similar to the respective HH modes. The frequency of the asymmetric NH stretching vibration, $Q_2^{HH}(B_u)$, is 2892 (2155) cm^{-1}.

For the asymmetric-substitution case, HD, we followed the same strategy. First, an explicit two-mode correlation potential was obtained comprising the two local stretching vibrations Q_1^{HD} and Q_2^{HD} and the strongly coupled low-frequency mode Q_6^{HD} (see Figure 5). Next, three more modes, $Q_3^{HD}Q_4^{HD}Q_5^{HD}$, were added after inspection of the third-order anharmonic force constants. As can be seen from Figures 5b–d, these modes involve skeleton rearrangements as well as substantial NH (Q_3^{HD},Q_4^{HD}) and ND (Q_5^{HD}) bending. The coupling constants exceeding 30 cm^{-1} are of two-mode origin, that is, $K_{113}^{HD}=-127$ cm^{-1}, $K_{223}^{HD}=75$ cm^{-1}, $K_{224}^{HD}=140$ cm^{-1}, and $K_{225}^{HD}=$

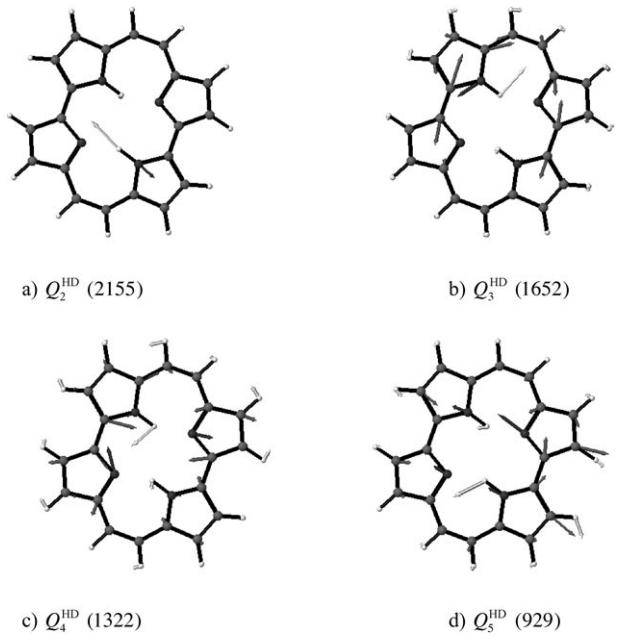

Figure 5. Selected normal-mode displacement vectors for the 6D model PES in the HD case. The harmonic frequencies are given in parentheses (in cm^{-1}). The frequency of the NH stretching mode, Q_1^{HD}, is 2892 cm^{-1}, whereas for the lowest frequency mode of the model, Q_6^{HD}, we have a value of 186 cm^{-1}.

$-139\ cm^{-1}$. The largest three-mode coupling is $K_{136}^{HD} = -23\ cm^{-1}$.

To calculate the ground-state wavefunction for the Hamiltonian, Equation (1), we employed the multiconfiguration time-dependent Hartree approach[33] together with imaginary time propagation[34] using the Adams–Bashforth–Moulton integrator, as implemented in the Heidelberg MCTDH program package.[35]

Results and Discussion

From Multidimensional Wavefunctions to the Geometric Isotope Effect

In Figure 6 we plot exemplary two-dimensional cuts of the multidimensional PES. For the HH and DD cases these cuts reflect the symmetry with respect to $Q_2^{HH/DD} = 0$ and $Q_3^{HH/DD} = 0$. This symmetry does not exist for the asymmetric (HD) substitution case. The anharmonic-mode coupling is obvious from the distortion of the PES with respect to the harmonic case. By virtue of the chosen normal-mode coordinate system, the minimum of the PES is at $Q = 0$, which corresponds to the equilibrium distance in the classical nuclei limit.

The ground-state probability distributions are also shown in Figure 6. Mere visual inspection already indicates that the maxima of these densities do not coincide with the PES minima, that is, they are shifted according to the distortion of the PES. In order to quantify this deviation we have calculated the expectation value of the model coordinates [in units of a_0 (a.m.u.)$^{1/2}$]: For the HH case we obtain: $\langle Q_1^{HH} \rangle = 0.07$, $\langle Q_2^{HH} \rangle = \langle Q_3^{HH} \rangle = 0.00$, and $\langle Q_4^{HH} \rangle = -0.48$, whereas for the DD case we have: $\langle Q_1^{DD} \rangle = 0.05$, $\langle Q_2^{DD} \rangle = \langle Q_3^{DD} \rangle = 0.00$, and $\langle Q_4^{DD} \rangle = -0.26$. For the asymmetric HD case, on the other hand, the expectation values of all coordinates differ from zero. We find: $\langle Q_1^{HD} \rangle = 0.04$, $\langle Q_2^{HD} \rangle = -0.05$, $\langle Q_3^{HD} \rangle = -0.01$, $\langle Q_4^{HD} \rangle = 0.02$, $\langle Q_5^{HD} \rangle = -0.01$, and $\langle Q_6^{HD} \rangle = -0.34$. Notice that these values reflect the combined effect of anharmonicity and quantum-mechanical zero-point energy.

In order to establish a link to the geometries, which are usually obtained from NMR experimental data, we have to translate these expectation values into geometric changes. This was done by displacing the equilibrium structures along the normal-mode coordinates according to these expectation values. From the so-obtained geometry we determined the

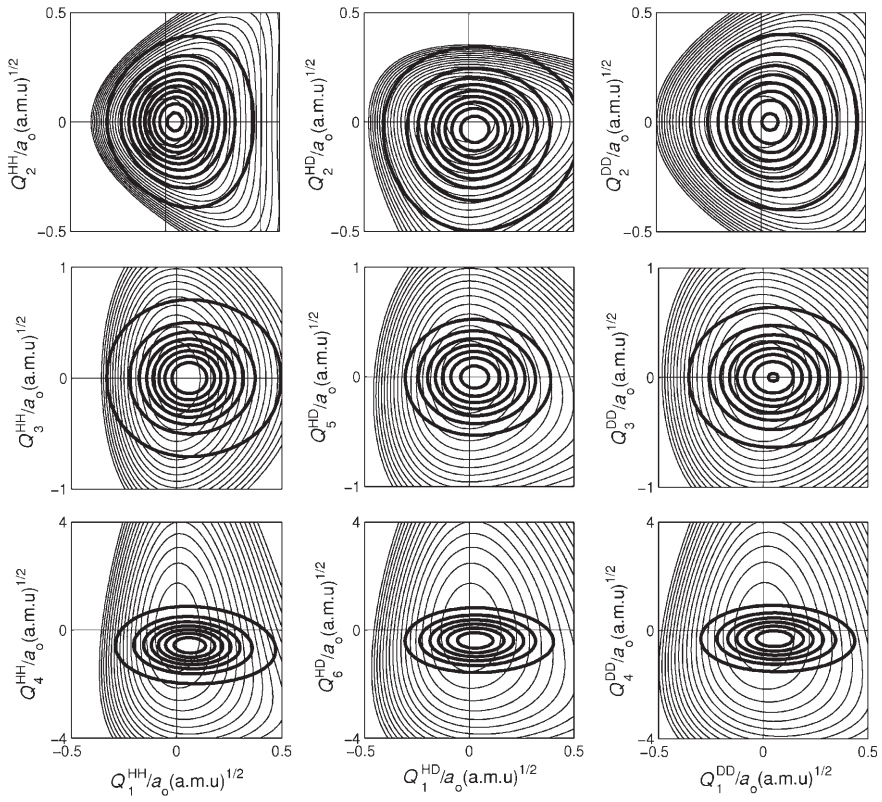

Figure 6. Exemplary cuts of the multidimensional PESs together with the respective ground-state vibrational probability density functions. The latter were obtained by using a harmonic-oscillator, discrete, variable representation on the following grid [in a_0 (a.m.u.)$^{1/2}$]: $Q_{1/2}^{HH/HD/DD}$ [−0.65:0.65] (64 points), $Q_3^{HH/HD/DD}$ [−1.5:1.5] (64 points), Q_4^{HD} [−1.5:1.5] (64 points), Q_5^{HD} [−1.5:1.5] (64 points), and $Q_4^{HH/DD}$, Q_6^{HD} [−6.5:6.5] (128 points). Contour spacing for the potential: 0.05–1 (in steps of 0.05 eV, first row) and 0.05–0.8 (in steps of 0.05 eV, second and third rows).

corresponding new bond distances which contain the quantum correction on the anharmonic PES.

Table 1 summarizes the hydrogen-bond parameters, R_{NH}, R_{NN}, $R_{N\cdots H}$, as well the NHN angle for the HH, HD, and DD cases. Comparing the HH and DD cases we observe the ordering: $R_{NH}^{class} < R_{NH}^{quant}(DD) < R_{NH}^{quant}(HH)$, $R_{N\cdots H}^{class} > R_{N\cdots H}^{quant}(DD) > R_{N\cdots H}^{quant}(HH)$, and $R_{NN}^{class} > R_{NN}^{quant}(DD) > R_{NN}^{quant}(HH)$ from which we can draw the following conclusions: The quantum effects lead to an elongation of the NH distances and an accompanying contraction of the NN distances. This simultaneous change reflects the multidimensionality of HB dynamics (cf. Figure 1 c) which in the present case leads to a bond that is stronger in the quantum case as compared to the classical one. Double deuteration causes the quantum effects to diminish, that is, the HB becomes weaker. In essence this is what is behind the so-called Ubbelohde or secondary GIE for HBs having a double minimum potential.

Table 1. HB parameters [Å and °] as calculated by the conventional method (classical nuclei) and from the coordinate expectation value on a four- and six-dimensional PES for HH/DD and HD, respectively.

	Classical	HH(4D)	HD (6D)		DD(4D)
			H	D	
R_{NH}	1.049	1.080	1.078	1.067	1.066
$R_{N\cdots H}$	1.678	1.622	1.630	1.642	1.649
R_{NN}	2.655	2.628	2.636	2.637	2.642
<NHN	152.8	152.6	152.8	152.8	152.7

Focusing on the case of single deuteration (HD), we observe that the distances R_{NH} change in a similar way to those in the HH and DD cases upon including quantum effects. On the other hand, the distances R_{NN} take values which are about the same for both HBs and which are intermediate between the HH and DD cases. In other words, *single substitution leads to a weakening of both HBs* as compared to the HH quantum case.

Comparison with NMR Experimental Results

In this section we compare our calculations with experimental data. Unfortunately, a direct measurement of geometric H/D isotope effects using X-ray diffraction is not precise enough to analyze tiny changes in HB geometries upon deuteration. Moreover, semideuterated samples would give only averaged distances over both N···H–N and N–D···N hydrogen bonds, which is insufficient for our study. Therefore, we used NMR as an indirect method to determine the GIE in the following way: In the first step, isotope effects on chemical shifts of bridging protons in porphycene as well as in three substituted porphycenes[36] were obtained. The ^1H and ^2H NMR spectra of partially deuterated porphycene and its derivatives were recorded, and the chemical shifts of different isotopomers, $\delta_{\underline{H}H}, \delta_{\underline{H}D}, \delta_{\underline{D}H}$, and $\delta_{\underline{D}D}$ were measured. In the second step, the NMR chemical shifts were correlated with the geometry parameters $q_1 = (r_1+r_2)/2$ and $q_2 = (r_1+r_2)$, as depicted in Figure 1 a. From Table 1 we recognize that the NHN angle is not much influenced by quantum effects and deuteration, that is, we can assume that $r_1 \approx R_{NH}$ and $r_2 \approx R_{N\cdots H}$.

Steiner obtained an experimental correlation between q_1 and q_2 based on neutron diffraction data for various N–H···N hydrogen bonds.[37,38] This relationship indicates that both parameters q_1 and q_2 are related to each other and cannot be varied independently. Limbach et al. modified this correlation and obtained a better fit to experimental data, especially in the region of symmetric and quasisymmetric hydrogen bonds (where q_1 is close to 0).[39] Knowing experimental X-ray geometries of porphycene and porphyrin, as well as N–H distances obtained from dipolar relaxation data,[16] and adapting an experimental model for the N–H···O hydrogen bond[40] to the N–H···N case, we can predict the primary H/D GIE. An established correlation of proton/deuteron chemical shifts and the geometric parameter q_1[16] made it possible to estimate the secondary H/D GIE as well. The q_1 and q_2 values obtained from this analysis, as well as those obtained from the theoretical model, are collected in Table 2.

Table 2. HB length $q_2 = (r_1+r_2)$ and hydrogen-transfer coordinate $q_1 = (r_1-r_2)/2$ obtained from NMR experimental results (the theoretical values according to Table 1 are shown in parenthesis).

	HH	HD		DD
		H	D	
q_1 [Å]	0.2500 (0.2700)	0.2559 (0.2750)	0.2656 (0.2870)	0.2706 (0.2905)
q_2 [Å]	2.7000 (2.7020)	2.7059 (2.7080)	2.7147 (2.7090)	2.7200 (2.7150)

Comparing experiment and theory in Figure 7 we should take into account the following points: 1) There are several sources of experimental errors arising from the deconvolution of the chemical-shift data, their correlation to q_1 values as well

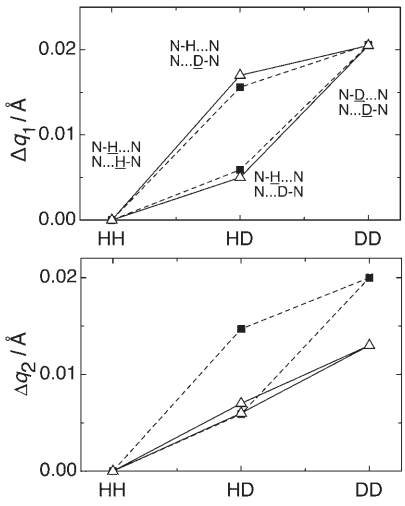

Figure 7. Comparison between theoretical (△) and experimental (■) values of the change of the HB parameters q_1 and q_2 with respect to the HH case. Notice that the experimental data points derive from the analysis of the chemical shifts $\delta_{\underline{H}H}, \delta_{\underline{H}D}, \delta_{\underline{D}H}$, and $\delta_{\underline{D}D}$.

as the q_1-q_2 correlation. 2) The level of quantum chemistry and the reduced dimensionality model introduce an error which is similar for all isotopomers, although difficult to quantify.

Consider the primary GIE, that is, the change of q_1 shown in the upper panel of Figure 7. Here, the agreement between theory and experiment is excellent. Notice that according to Table 2, there is a rather small offset of 0.02 Å between the absolute values. The predicted value of q_2 for the HH case coincides almost quantitatively with the experiment (cf. Table 2). As far as the secondary GIE (i.e. the change of q_2) is concerned, the shift for DD essentially agrees within the expected error limits. For the HD case, theory predicts a rather concerted expansion of both HBs. The experimental data indicate the same cooperativeness although the expansion is not as symmetric. Nevertheless, the overall agreement between experiment and theory is rather satisfactory, thus substantiating the conclusion that the two intramolecular HBs in porphycene are behaving cooperatively.

Conclusions

Combining quantum chemical PES calculations with a multiconfiguration time-dependent Hartree solution of the nuclear Schrödinger equation, the multidimensional ground-state wavefunction for the double HB in porphycene was investigated. As a consequence of the combined effect of zero-point energy and anharmonic mode coupling, the expected values of the interatomic distances deviate strongly from classical predictions giving rise to a quantum mechanically induced strengthening of the HBs. Since the zero-point energy depends on the nuclear masses, one observes an isotope dependence of the HB distances, that is, the HB strength is modified. Comparing this geometric isotope effect for symmetric (HH/DD) and asymmetric (HD) isotopomers it was found that even a single substitution already causes a simultaneous contraction of both HBs.

The theoretical predictions were confirmed by NMR experimental data. For the primary geometric isotope effect we found a good agreement between theory and experiment. Although this agreement deteriorates for the secondary geometric isotope, the comparison is still reasonably good, in particular if one takes into account possible experimental and theoretical errors. Thus, we can conclude that the two HBs in porphycene are cooperative.

In summary, we demonstrated that geometric isotope effects can, in principle, be used to address the issue of cooperativity of coupled intramolecular HBs. The favorable—almost quantitative—comparison between experiment and theory for a system of this size is rather encouraging. Returning to our working hypothesis, our findings for porphycene do not yet support the conclusion that the cooperativity expressed in the geometrical changes also leads to a preference for concerted double hydrogen transfer. To address this point and to establish a firm relation between the quantum effects on the geometry and the kinetics, as well as the dynamics of HBs, further studies are necessary.

Acknowledgements

This work was financially supported by the Deutsche Forschungsgemeinschaft (project Ma 515/20-2).

Keywords: anharmonicity · hydrogen bonds · isotope effects · molecular dynamics · vibrational wavefunction

[1] *Isotope effects in chemistry and biology* (Eds.: A. Kohen, H.-H. Limbach), Taylor and Francis, Boca Raton, **2005**.
[2] P. E. Hansen, *Isotope Effects on Chemical Shifts as a Tool in Structural Studies*, Roskilde University Press, Roskilde, **1996**.
[3] H. Benedict, H.-H. Limbach, M. Wehlan, W.-P. Fehlhammer, N. S. Golubev, R. Janoschek, *J. Am. Chem. Soc.* **1998**, *120*, 2939.
[4] I. G. Shenderovich, H.-H. Limbach, S. N. Smirnov, P. M. Tolstoy, G. S. Denisov, N. S. Golubev, *Phys. Chem. Chem. Phys.* **2002**, *4*, 5488.
[5] N. S. Golubev, S. N. Melikova, D. N. Shchepkin, I. G. Shenderovich, P. M. Tolstoy, G. S. Denisov, *Z. Phys. Chem.* **2003**, *217*, 1549.
[6] J. Stare, A. Jezierska, G. Ambrožič, I. Košir, J. Kirdič, A. Koll, J. Mavri, D. Hadži, *J. Am. Chem. Soc.* **2004**, *126*, 4437.
[7] H.-H. Limbach, O. Klein, J. M. L. d. Amo, J. Elguero, *Z. Phys. Chem.* **2004**, *218*, 17.
[8] R. D. Levine, *Molecular Reaction Dynamics*, Cambridge University Press, Cambridge, **2005**.
[9] J. P. Klinman, *Pure Appl. Chem.* **2003**, *75*, 601.
[10] S. J. Benkovic, S. Hammes-Schiffer, *Science* **2003**, *301*, 1196.
[11] J. E. Del Bene in *Isotope effects in chemistry and biology* (Eds.: A. Kohen, H.-H. Limbach), Taylor and Francis, Boca Raton, **2005**, p. 153.
[12] S. N. Smirnov, N. S. Golubev, G. S. Denisov, H. Benedict, P. Schah-Mohammedi, H.-H. Limbach, *J. Am. Chem. Soc.* **1996**, *118*, 4094.
[13] A. R. Ubbelohde, K. J. Gallagher, *Acta Crystallogr.* **1955**, *8*, 71.
[14] G. A. Jeffrey, *An Introduction to Hydrogen Bonding*, Oxford University Press, New York, **1997**.
[15] D. F. Brougham, R. Caciufoo, A. J. Horsewill, *Nature* **1999**, *397*, 241.
[16] U. Langer, C. Hoelger, B. Wehrle, L. Latanowicz, E. Vogel, H.-H. Limbach, *J. Phys. Org. Chem.* **2000**, *13*, 23.
[17] P. M. Tolstoy, P. Schah-Mohammedi, S. N. Smirnov, N. S. Golubev, G. S. Denisov, H.-H. Limbach, *J. Am. Chem. Soc.* **2004**, *126*, 5621.
[18] E. Vogel, M. Köcher, H. Schmickler, J. Lex, *Angew. Chem.* **1986**, *98*, 262; *Angew. Chem. Int. Ed.* **1986**, *25*, 257.
[19] T. Malsch, G. Hohlneicher, *J. Phys. Chem. A* **1997**, *101*, 8409.
[20] B. Wehrle, H.-H. Limbach, M. Köcher, O. Ermer, E. Vogel, *Angew. Chem.* **1987**, *99*, 914; *Angew. Chem. Int. Ed.* **1987**, *26*, 934.
[21] J. Waluk in *Hydrogen-Transfer Reactions, Vol. 1.: Physical and Chemical Aspects* (Eds.: J. T. Hynes, J. P. Klinman, H.-H. Limbach, R. L. Schowen), Wiley-VCH, Weinheim, **2006**, p. 245.
[22] T. Malsch, M. Roeb, V. Karuth, G. Hohlneicher, *Chem. Phys.* **1998**, *227*, 331.
[23] P. M. Kozlowski, M. Z. Zgierski, J. Baker, *J. Chem. Phys.* **1998**, *109*, 5905.
[24] J. Almlöf, *Chem. Phys. Lett.* **1972**, *17*, 49.
[25] M. Tachikawa, M. Shiga, *J. Am. Chem. Soc.* **2005**, *127*, 11 908.
[26] M. F. Shibl, M. Tachikawa, O. Kühn, *Phys. Chem. Chem. Phys.* **2005**, *7*, 1368.
[27] Gaussian 03, M. J. Frisch, G. W. Trucks, H. B. Schlegel, G. E. Scuseria, M. A. Robb, J. R. Cheeseman, J. A., Jr., Montgomery, T. Vreven, K. N. Kudin, J. C. Burant, J. M. Millam, S. S. Iyengar, J. Tomasi, V. Barone, B. Mennucci, M. Cossi, G. Scalmani, N. Rega, G. A. Petersson, H. Nakatsuji, M. Hada, M. Ehara, K. Toyota, R. Fukuda, J. Hasegawa, M. Ishida, T. Nakajima, Y. Honda, O. Kitao, H. Nakai, M. Klene, X. Li, J. E. Knox, H. P. Hratchian, J. B. Cross, V. Bakken, C. Adamo, J. Jaramillo, R. Gomperts, R. E. Stratmann, O. Yazyev, A. J. Austin, R. Cammi, C. Pomelli, J. W. Ochterski, P. Y. Ayala, K. Morokuma, G. A. Voth, P. Salvador, J. J. Dannenberg, V. G. Zakrzewski, S. Dapprich, A. D. Daniels, M. C. Strain, O. Farkas, D. K. Malick, A. D. Rabuck, K. Raghavachari, J. B. Foresman, J. V. Ortiz, Q. Cui, A. G. Baboul, S. Clifford, J. Cioslowski, B. B. Stefanov, G. Liu, A. Liashenko, P. Piskorz, I. Komaromi, R. L. Martin, D. J. Fox, T. Keith, M. A. Al-Laham, C. Y. Peng, A. Nanayakkara, M. Challacombe, P. M. W. Gill, B. Johnson, W. Chen, M. W. Wong, C. Gonzalez, J. A. Pople, Gaussian Inc., Wallingford CT, **2003**.

[28] J. Sepioł, Y. Stepanenko, A. Vdovin, A. Mordziński, E. Vogel, J. Waluk, *Chem. Phys. Lett.* **1998**, *296*, 549.
[29] M. F. Shibl, *PhD Thesis*, Freie Universität, Berlin, **2006**.
[30] J. K. G. Watson, *Mol. Phys.* **1968**, *15*, 479.
[31] S. Carter, S. J. Culik, J. M. Bowman, *J. Chem. Phys* **1997**, *107*, 10458.
[32] W. Schneider, W. Thiel, *Chem. Phys. Lett.* **1989**, *157*, 367.
[33] H.-D. Meyer, G. A. Worth, *Theor. Chem. Acc.* **2003**, *109*, 251.
[34] R. Kosloff, H. Tal-Ezer, *Chem. Phys. Lett.* **1986**, *127*, 223.
[35] G. A. Worth, M. Beck, A. Jäckle, H.-D. Meyer, *MCTDH 8.3 ed.*, University of Heidelberg, Heidelberg, **2003**.
[36] A. Ghosh, J. Moulder, M. Bröring, E. Vogel, *Angew. Chem.* **2001**, *113*, 445; *Angew. Chem.* **2001**, *40*, 431.
[37] T. Steiner, *J. Chem. Soc., Chem. Commun.* **1995**, 1331.
[38] T. Steiner, *J. Phys. Chem. A* **1998**, *102*, 7041.
[39] H.-H. Limbach, M. Pietrzak, H. Benedict, P. M. Tolstoy, N. S. Golubev, G. S. Denisov, *J. Mol. Struct.* **2004**, *706*, 115.
[40] H.-H. Limbach, M. Pietrzak, S. Sharif, P. M. Tolstoy, I. G. Shenderovich, S. N. Smirnov, N. S. Golubev, G. S. Denisov, *Chemistry Eur. J.* **2004**, *10*, 5195.

Received: August 18, 2006
Published online on December 19, 2006

